processes

MDPI

Article

Numerical Simulation Study on Vibration Reduction Effect of Flexible Cutting-Tooth Unit

Haitao Ren [1,2,*], Jingwei Xu [1], Xin Jia [1], Sheng Zhou [1], Chunxiao Zhou [1], Yingxin Yang [1,2] and Qi Zhan [1]

[1] School of Mechanical and Electrical Engineering, Southwest Petroleum University, Chengdu 610500, China; xujw844816022@163.com (J.X.); 13408553630@163.com (X.J.); 17746722615@163.com (S.Z.); 19180876620@163.com (C.Z.); yangyx36@163.com (Y.Y.); philcoulson2000@163.com (Q.Z.)

[2] National Engineering Laboratory of Oil and Gas Drilling Technology, Rock Breaking and Drill Bit Institute, Southwest Petroleum University, Chengdu 610500, China

* Correspondence: renhaitao781026@163.com

Abstract: Under the conditions of drilling in gravel-bearing and heterogeneous stratas, the movement and force of the PDC bit during drilling are highly unstable. Irregular impact loads often cause fatigue failures such as tooth fracture, tooth breakage and delamination of the composite sheet. Dynamic impact load is the main cause of fatigue failure of cutting-tooth, which seriously affects the rock-breaking performance of PDC bits. This paper proposes a flexible cutting tooth unit consisting of a central tooth, an elastic element, and a base. The technical concept of flexible-cutting rock breaking is to reduce the impact load amplitude suffered during the cutting process to a certain threshold range by setting elastic elements or reducing the support stiffness of the cutting tooth, so as to inhibit the expansion of micro defects caused by the impact dynamic load of cutting teeth and prolong the service life of drill bits. The finite-element models of flexible cutting teeth for rock cutting were established. The influence of cutting depth, front rake angle and stiffness of elastic elements on the cushioning and vibration-absorption effect of flexible cutting was analysed. The results show that flexible cutting can reduce the peak and average value of von Mises stress at the cutting edge. Under different cutting-depth conditions, the decline rates were 21.45–49.02% and 9.42–17.8%, respectively. Then, under different front-rake-angle conditions, the decline rates were 20.51–24.02% and 9.41–17.8%, respectively. There is a suitable stiffness of the elastic element, which makes the peak and average value of von Mises stress at the cutting edge of the flexible cutting-tooth unit perform better and the effect of improving the uneven stress distribution at the cutting edge better. Flexible cutting technology can effectively improve the adaptability of the PDC bit in heterogeneous formations and reduce the occurrence of abnormal failure of cutting teeth. The research results of this paper can provide theoretical support for the drilling speed of PDC bits in hard formations.

Keywords: PDC bit; rock breaking mechanism; flexible cutting; drilling speed; impact dynamic load

Citation: Ren, H.; Xu, J.; Jia, X.; Zhou, S.; Zhou, C.; Yang, Y.; Zhan, Q. Numerical Simulation Study on Vibration Reduction Effect of Flexible Cutting-Tooth Unit. *Processes* **2023**, *11*, 2658. https://doi.org/10.3390/pr11092658

Academic Editors: Yinhui Zuo and Hui Han

Received: 14 August 2023
Revised: 28 August 2023
Accepted: 31 August 2023
Published: 5 September 2023

1. Introduction

Compared with the roller bit, there are some significant advantages in terms of aggression and anti-abrasion of the PDC bit, which can effectively improve the penetration rate and drilling efficiency. However, when drilling in heterogeneous or hard formations, the movement and force of the drill bit are very unstable and the cutting teeth are subjected to irregular impact loads, causing fatigue failures such as tooth breakage, tooth fracture and delamination of the composite sheet [1–3]. The service life is greatly reduced, the number of trips is increased, and the efficient development of oil and gas resources is hindered.

Experts and scientists at home and abroad have carried out a lot of research to propose a variety of solutions to reduce the adverse effects of vibration, improve the cushioning and vibration-absorption capacity of the cutting teeth, and prevent the impact failure of the drill bit. The researchers enhanced the impact resistance of the drill bit by changing

the shape of the composite sheet and designing the special-shaped teeth individually [4]. Durrand et al. [5] invented a new type of PDC tooth, namely conical tooth. The shape of the tooth is conical, the thickness of the diamond layer at the top of the cone is twice that of the conventional PDC tooth, and the impact resistance and wear resistance are increased by 100% and 25%, respectively. Zhao et al. [6,7] proposed roof-shaped and three-edge-shaped cutting teeth. According to laboratory tests, the impact resistance of the two types of shaped teeth has been improved to a certain extent compared with flat teeth. Liu et al. [8] analysed the rock-breaking mechanism of non-planar triangular teeth by numerical simulation. It was found that the non-planar triangular tooth has less tangential force than the cylindrical tooth when breaking rock, and has greater impact resistance and wear resistance. Then, the bonding surface between the carbide matrix and the diamond layer of the conventional PDC teeth is planar, such that the PDC interface bond is weak [9], which is acceptable as a cutting tool, but slightly insufficient in terms of impact resistance when used as a drilling tool. Johnson et al. [10] developed a cemented carbide substrate with a serrated interface. The serrated interface makes the polycrystalline diamond (PCD) layer thicker at the outer edge of the PDC tooth, and the serrated structure can also disperse the interfacial stress, reducing the possibility of cracking or delamination of the polycrystalline diamond compacts during temperature changes or severe shocks. Gao et al. [11] used tree rings as bionic prototypes to design the interface structure of bionic PDC teeth. Such a structural design fully guarantees the stability and firmness of the interface. Yang [12] designed a PDC with a rectangular protrusion interface. The rectangular protrusion can shift the maximum shear stress from the edge of the interface to the inside of the diamond, thereby reducing the possibility of spalling of the composite sheet under impact. For the whole PDC bit, it is also possible to comprehensively consider various design parameters and optimise the design of the bit structure to improve impact resistance and achieve drilling speed. Han et al. [13] developed a "triangular teeth + bevel teeth + flat teeth" drill. It not only has the strong aggressiveness of the general conventional PDC bit, and maintains high mechanical drilling speed and fast drilling, but also has strong impact resistance and anti-abrasion ability. Wang et al. [14] optimised the structure of the drill bit, such as reasonable selection of the number of the blades, and optimisation of the tooth structure and crown profile to improve the impact resistance and anti-abrasion performance of the drill bit. In addition, the cutting-depth control of the cutting teeth [15–20] (DOC) is also one of the main means of reducing vibration and improving the impact resistance of the drill bit. It controls the cutting depth by determining the height difference between the teeth, thereby reducing torque fluctuations and improving dynamic stability.

The above technology shows that unitisation, compatibility, and self-adaptation will be the development direction of PDC bits to improve impact resistance in the future. Therefore, this paper proposes a flexible cutting-tooth unit consisting of a central tooth, an elastic element, and a base. The elastic element behind the tooth interacts with the load, which can play its role of buffering and absorbing vibration, preventing overload impact damage and fatigue damage to the diamond layer. The flexible cutting-tooth unit is small in size and can be widely used. It is highly compatible with the previous impact-resistance technology and solves the dynamic response problem of cutting-depth control technology. The flexible cutting-tooth unit has wide development prospects. In this paper, the finite-element software Abaqus is used to establish the rock-breaking model of the flexible cutting-tooth unit and to study the effect of cutting depth, rake angle and elastic element stiffness on the von Mises stress at the cutting edge. The research can support the technical application of flexible vibration-reduction cutting technology, which can also improve drilling efficiency, reduce drilling costs, and shorten the development cycle of deep, complex, and difficult drilling formations.

2. Vibration-Reduction Mechanism of Flexible Cutting Technology

As the hardness and plasticity of the rock in deep formations increases, the abrasiveness is increased and the drillability is poor. The drill bit is prone to vibration in these

well sections [21–23]. The shear stress in the shear plane of the rock is not sufficient to overcome the frictional resistance, so the drill bit initially stops rotating on the rock until the torque and energy transmitted by the drill string continue to the moment the rock can be broken. The energy explodes instantaneously, which increases the stress on the tooth surface, intensifying the impact between the composite layer and the rock layer, and ultimately causing fatigue failure such as tooth breakage, tooth fracture and delamination, as shown in Figure 1.

Figure 1. Abnormal failure forms such as PDC tooth breakage and delamination. (Scale on the left: 2:1).

The flexible cutting-tooth unit consists of a central tooth, an elastic element, and a base. As shown in Figure 2, the PDC bit is provided with a tooth hole for installation of the flexible cutting-tooth unit, which is installed in the tooth hole. The base is fixed to the tooth hole by welding, interference fit, threaded connection, etc. [24]. The three paths of action on the cushioning and vibration absorption effect of the flexible cutting tooth unit are shown in Figure 3. First of all, in large-depth cutting, the excessive tangential force along the axial component of the cutting-tooth will squeeze the elastic element and cause the central tooth to retreat to a certain extent, which is called the tolerance phenomenon of flexible cutting. In the longitudinal direction, the cutting depth is reduced, which helps to reduce the cutting stress on the tooth surface. Then, on the PDC bit equipped with a flexible cutting tooth unit, when the cutting tooth collides violently with the formation, the huge instantaneous stress will also cause the flexible cutting-tooth unit to retreat. The local stress originally carried by a single cutting tooth is now carried by multiple cutting teeth to achieve a corresponding reduction in tooth surface stress. In addition, when the elastic element plays a role, the process of changing its thickness will prolong the cutting time, slow down the cutting speed, and then reduce the impact dynamic load increment. As shown in Figure 4, by reducing the stress loaded on the part, the number of stress cycles in the part is increased. In other words, the service life of the part is increased.

In conclusion, from the above three paths of action in Figure 3 and the fatigue life curve of the classical material in Figure 4, it can be learned that flexible cutting reduces the load on the PDC tooth and can moderately increase its service life.

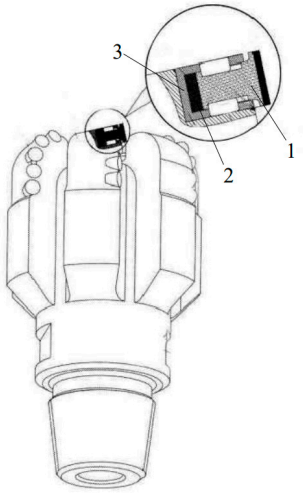

Figure 2. PDC bit with flexible cutting-tooth unit. (Scale: 1:8) 1—The central tooth, 2—The elastic element, 3—The base.

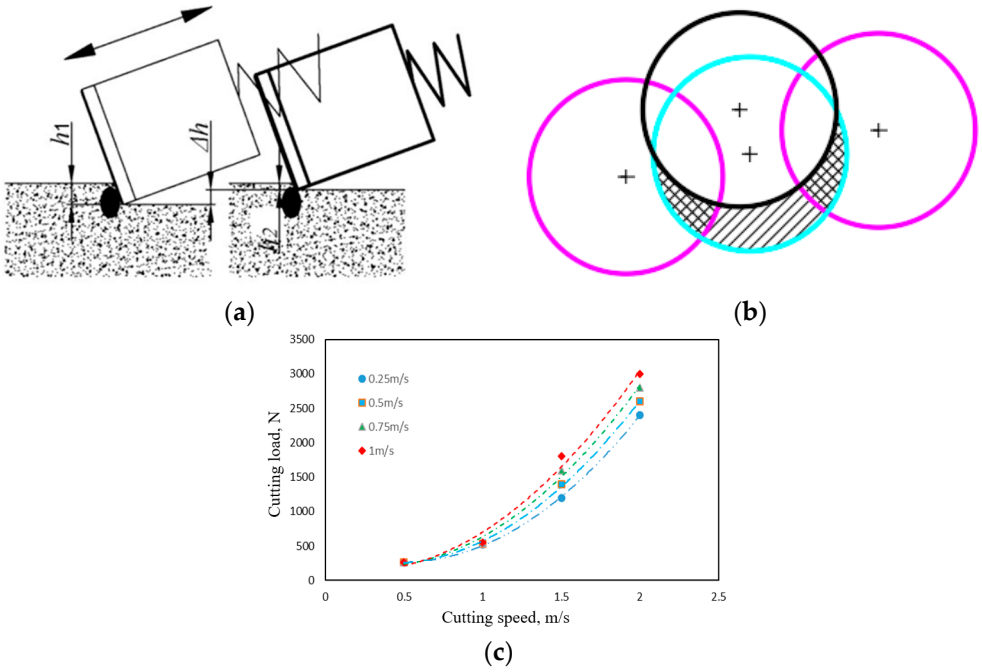

Figure 3. Action Paths of Flexible Cutting-Tooth Unit. (**a**) Reduce cutting depth (Scale: 1:1) (**b**) Increase the number of teeth involved in cutting (Scale: 1.5:1) (**c**) Reduce impact dynamic load.

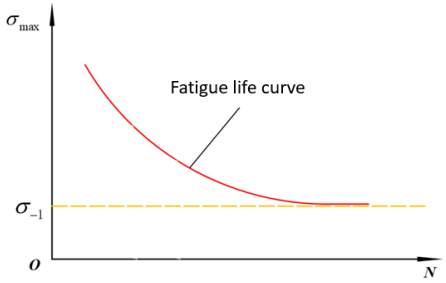

Figure 4. Classical Material Fatigue Life Curve.

3. Numerical Simulation

The model of the interaction between the flexible cutting-tooth element and the rock is shown in Figure 5. In the drilling process of the PDC bit, the flexible cutting tooth unit moves linearly along the drilling direction of the bit while performing a rotary motion around the central axis of the bit. But the change in bit feed depth is small after a week of rotation, so the trajectory of the flexible cutter unit in the drilling process can be simplified to a linear motion with a fixed cutting depth.

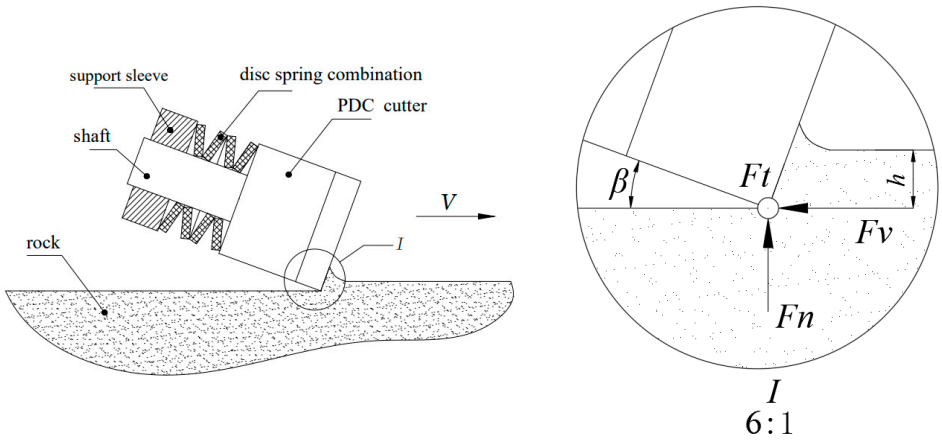

Figure 5. Model of Interaction between Flexible Cutting-Tooth Unit and Rock. (Scale on the left: 1:1).

In the process of breaking rock, the force of the cutting teeth can be divided into tangential force F_v, axial force F_n and radial force F_t. The direction of F_v is opposite to the direction of cutting speed, the direction of F_n and F_t are perpendicular to each other, and the direction of F_t is perpendicular to the paper surface. As shown in Figure 5, β is the front rake angle of the cutting tooth, h is the penetration depth of the cutting tooth. The disc-spring combination is the elastic element used. The support sleeve is the base.

3.1. Constitutive Relation of Rock

Since the plastic failure of rock cannot be recovered, the plastic constitutive relation of rock, also known as the rock strength criterion, is the failure criterion of rock. The Drucker–Prager criterion (D-P criterion) is a combination of the Mohr–Coulomb criterion and the von Mises criterion, which are extended and modified. The D-P criterion can take into account the influence of the intermediate principal stress and hydrostatic pressure on the rock strength and reflect the expansion phenomenon caused by the shearing process of the rock. The D-P criterion uses the normal stress (σ_{oct}) and shear stress (τ_{oct}) on the octahedral surface to express the influence of the intermediate principal stress (σ_2) on the rock breaking [25], i.e.,

$$\tau_{\text{oct}} = \tau_0 + m\sigma_{\text{oct}} \tag{1}$$

In the formula,

$$\begin{cases} \tau_{\text{oct}} = \frac{1}{3}\sqrt{(\sigma_1-\sigma_2)^2+(\sigma_2-\sigma_3)^2+(\sigma_3-\sigma_1)^2} \\ \sigma_{\text{oct}} = \frac{1}{3}(\sigma_1+\sigma_2+\sigma_3) \\ m = -\sqrt{6}\alpha \\ \tau_0 = \frac{\sqrt{6}}{3}k \end{cases} \tag{2}$$

In the formula, $\sigma_1, \sigma_2, \sigma_3$ are the maximum principal stress, intermediate principal stress and minimum principal stress of the rock, respectively. α, k are the experimental constants related to the cohesion ξ and internal friction angle C of the rock.

The change of stress Lode angle θ_σ will affect the stress–strain relationship of the rock.

When $\theta_\sigma = \frac{\pi}{6}$, the rock is compressed and hardened. It can be obtained that,

$$\alpha = \frac{2\sin\xi}{\sqrt{3}(3-\sin\xi)}, k = \frac{6\cos\xi}{\sqrt{3}(3-\sin\xi)} \tag{3}$$

When $\theta_\sigma = -\frac{\pi}{6}$, the rock is stretched and hardened, it can be obtained that,

$$\alpha = \frac{2\sin\xi}{\sqrt{3}(3+\sin\xi)}, k = \frac{6\cos\xi}{\sqrt{3}(3+\sin\xi)} \tag{4}$$

When $\tan\theta_\sigma = -\frac{\sin\xi}{\sqrt{3}}$, the rock is sheared and hardened. It can be obtained that,

$$\alpha = \frac{\sqrt{3}\sin\xi}{3\sqrt{3+\sin^2\xi}}, k = \frac{\sqrt{3}c\cos\xi}{\sqrt{3+\sin^2\xi}} \tag{5}$$

3.2. Establishment of the Numerical Models

The variable parameters involved in the simulation experiment of the flexible cutting tooth unit are the cutting depth, the front rake angle and the stiffness of the elastic element. In particular, in order to make the stiffness change of the elastic element consistent with the real situation, the disc spring is specifically used as the elastic element that exists in reality. Three types of disc springs A, B and C were purchased. By changing their number, they are combined to achieve the change in stiffness. For example, the disc-spring combination of type A4 means that four disc springs of type A are used as elastic elements. The stiffness of the disc-spring combination is equal to the stiffness of the elastic element, so it is necessary to test the stiffness of different disc-spring combinations. And since the stiffness of the disc-spring is non-linear, the results of the stiffness test are mathematically fitted. Finally, the load–displacement relationship of various disc-spring combinations is obtained to characterise their stiffness. The load–displacement relationship of various disc-spring combinations is shown in Table 1. It can be seen that the stiffness of disc-spring combinations A2, A4, B4 and C4 gradually decreases.

Table 1. Mathematical expression of stiffness.

The Combination of Disc Springs	The Expression of the Relationship between Load and Displacement	
A2	$y = 2.0483x - 0.0304$	$R^2 = 0.9987$
A4	$y = 1.02415x - 0.0304$	$R^2 = 0.9987$
B4	$y = 0.49795x - 0.0236$	$R^2 = 0.9996$
C4	$y = -0.0788875x^2 + 0.442575x - 0.0738$	$R^2 = 0.9948$

Notes: y is load/kN; x is displacement/mm.

A simplified finite element analysis model of the rock breaking of the flexible cutting-tooth unit is established by using finite element software Abaqus. The size of the cutting part of the cutting tooth model is ϕ 19 mm × 13 mm. The cutting stroke is appropriately extended to observe the obvious phenomenon of rock breaking and vibration reduction, so the size of the rock model is set to 110 × 60 × 20 mm. The rock and cutting teeth are meshed by "hexahedral element" (C3D8R) with high calculation accuracy and high stability, and the Druker–Prager failure criterion is used in the failure stage. In order to improve the accuracy and speed of the calculation, the area of interaction between the rock and the cutting teeth is refined by mesh refinement. The sensitivity of the mesh is checked. When the number of elements continues to increase, it no longer has a greater impact on the calculation results of the model. Therefore, the number of elements in this paper is set to 688,792. The cutting model with a disc-spring combination behind the cutting teeth is called a flexible cutting model. Correspondingly, the conventional cutting model with a rigid sleeve behind the cutting teeth is called a rigid cutting model. The meshing of

the flexible cutting-tooth element and the rigid cutting tooth is shown in Figure 6. The complete scraping model is shown in Figure 7.

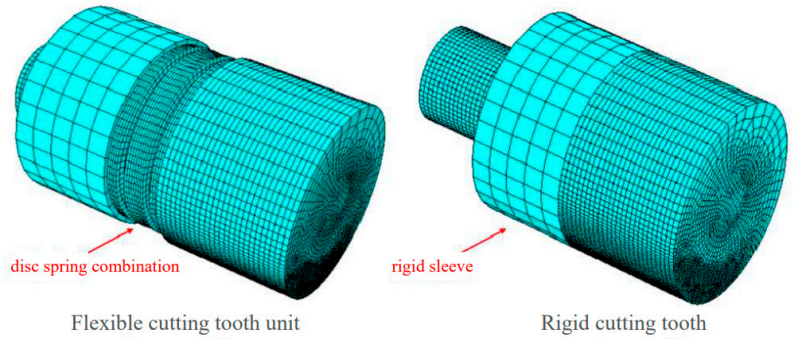

Figure 6. Mesh division of flexible cutting-tooth unit and rigid cutting tooth. (Scale: 1.5:1).

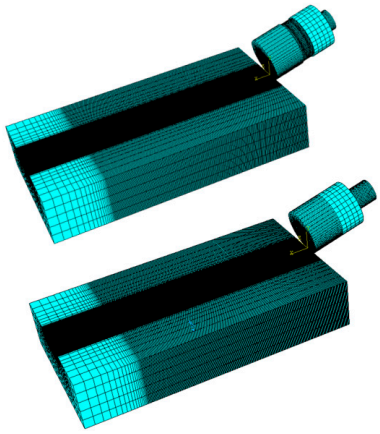

Figure 7. Flexible and rigid cutting model. (Scale: 1:3).

In this paper, the simulation experiment is carried out by using the method of control variables. The benchmark variables are a preset cutting depth of 1.5 mm, front rake angle of 15°, A4 disc-spring combination, and limestone rock (hard rock). Among them, in the cutting-depth variable, a preset cutting depth must first be set. As the tolerance phenomenon occurs during the operation of the flexible cutting-tooth unit, the actual cutting depth is often less than or equal to the preset cutting depth. Through the process output of Abaqus software, the actual cutting depth of the flexible cutting-tooth unit after stable operation is obtained, and the cutting depth of the subsequent rigid-cutting control group is set according to the actual cutting depth of the flexible cutting. The experimental scheme of the numerical simulation is shown in Table 2.

In the above simulation model, the material properties of the PDC cutter part are defined as the material properties of its diamond layer, and limestone is selected as the rock material. The elastic element benchmark selects the A4 disc spring combination as the flexible damping element setting. The rigid sleeve and the small section shaft behind the tooth adopt tungsten carbide as the material property. The material input parameters are shown in Table 3. Fixed boundary conditions are applied to the bottom, both sides and back of the rock, and fixed constraints in the Z direction are applied to the cutting teeth so that they can only move in the X and Y directions. The support sleeve is applied in an X direction at a speed of 0.25 m/s, and the degree of freedom in other directions is 0. The contact property between rock and cutting teeth adopts “general contact”. The contact between the disc spring and the disc spring and other parts is set to surface-to-surface contact(explicit). The contact between the shaft and other parts is also set to surface-to-surface contact(explicit). “Penalty” is selected as the “Friction formulation” and given the value “0.2”.

Table 2. Numerical Simulation Scheme.

Programme	Front Rake Angle β (°)	Type of Support	Preset Cutting Depth h (mm)
Change the cutting depth	15	A4 disc-spring combination rigid sleeve	1, 1.3, 1.5, 1.8, 2 The corresponding actual cutting depth
Change the front rake angle	5, 10, 20, 25	A4 disc-spring combination rigid sleeve	1.5 The corresponding actual cutting depth
Change the disc spring combination	15	A2, A4, B4, C4 disc-spring combinations rigid sleeve	1.5 The corresponding actual cutting depth

Table 3. Input parameters of the material.

Material	Elastic Modulus (MPa)	Poisson's Ratio	Tensile Strength (MPa)	Shearing Strength (MPa)	Internal Friction Angle (°)	Compressive Strength (MPa)	Plasticity Coefficient
Limestone rock	31,200	0.171	6.758	17.12	43.62	105.951	1.32
A4 disc-spring combination	206,000	0.3					
Cemented carbide	579,000	0.22					
Polycrystalline diamond	890,000	0.07					

3.3. Verification of the Numerical Models

In order to ensure the reliability of the numerical results, it is necessary to verify the established simulation model. Hence, before the numerical simulation, some laboratory single-tooth experiments of the flexible cutting unit with the front rake angle of 15°, A4 disc-spring combination, and limestone rock were carried out. As shown in Figure 8, the experimental facilities use the improved shaping machine of the Drill Research Institute of Southwest Petroleum University. The equipment has a constant speed and can meet the requirements of a single-tooth.

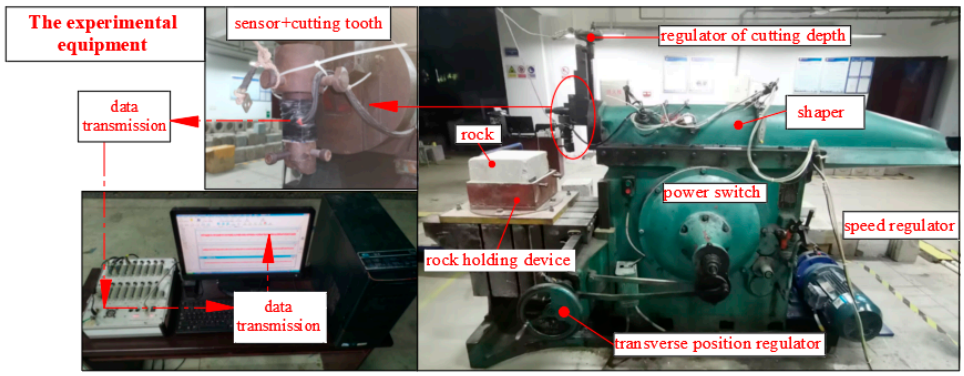

Figure 8. Single-tooth cutting rock-breaking experimental device.

The three-direction sensor is installed on the tool holder of the shaping machine. The cutting-tooth and the tooth seat are fixed on the sensor through two bolts. The cutting tooth is fixed on the tooth seat through the thread designed behind the tooth seat and on the cutting tooth matrix. Firstly, the rock is fixed on the cutting platform by the clamping device before the test, and the surface of the rock sample is smoothed by ordinary PDC teeth. Then, the flexible cutting-tooth unit and the rigid cutting tooth used in the test are installed on the sensor in order. The movement of the planer tool holder drives the cutting

teeth to scrape the rock in a straight line along the cutting direction. Next, the depth of the flexible cutting scratches is measured. Finally, the corresponding rigid cutting is performed according to the measured depth. The cutting force on the cutting teeth during the rock breaking process is obtained by the data acquisition system. Part of the operation process is shown in Figure 9.

(**a**) (**b**)

Figure 9. Part of the operation process. (**a**) Installation of gear seat (**b**) Measurement of cutting depth.

The actual cutting depth of the numerical simulation and experiment were compared. As shown in Figure 10, the experimental data of the actual cutting depths of flexible cutting under the conditions of 1 mm, 1.3 mm, 1.5 mm, 1.8 mm and 2 mm preset cutting depth were basically consistent with the simulation data.

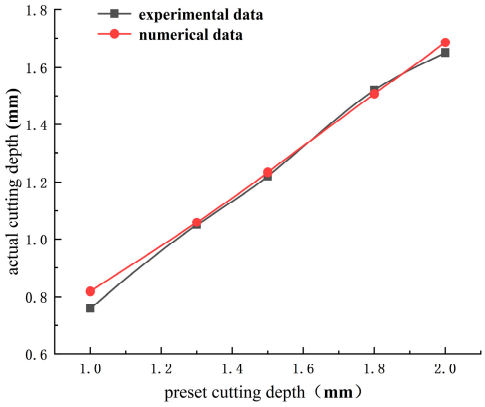

Figure 10. Comparison of Flexible Cutting Simulation and Experimental Cutting Depth Data.

The load magnitude of the numerical simulation and the laboratory test were compared. As shown in Figure 11, when the preset cutting depth is set to 1 mm, the average values of the experimental data and simulation data are 451.49 N and 487.17 N, respectively. The error range between the two is 7.9%. When the preset cutting depth is set to 1.5 mm, the average values of the experimental and simulation data are 689.98 N and 747.84 N, respectively. The error between them is 8.4%. When the preset cutting depth is set to 2 mm, the average values of the experimental data and simulation data are 895.4 N and 977.92 N, respectively. The error between the two is 9.2%. Considering that the numerical model cannot fully simulate the real heterogeneous rock, the dynamic randomness of rock breaking and the error of the sensor, the error of the simulation model is within the acceptable range. The flexible cutting simulation has a certain reference value.

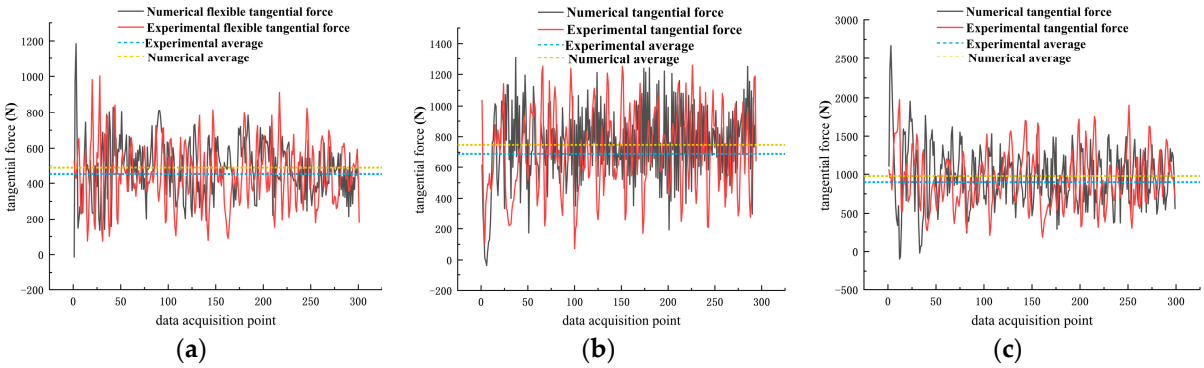

Figure 11. Comparison of Flexible Cutting Numerical and Experimental Cutting Load Data. (**a**) 1 mm (**b**) 1.5 mm (**c**) 2 mm.

4. Analysis of Simulation Results

In the process of scraping, the cutting teeth will peel off from the rock body, and form a small range of space without rock at the moment of leaving. At this time, the cutting tooth is in a state of no load. When it touches the rock again, it will be subjected to a reaction force of the rock, that is, the impact load in the model. The von Mises criterion is a yield criterion proposed by von Mises in 1913. The von Mises criterion is a comprehensive concept that considers the first, second and third principal stresses and can be used to evaluate fatigue failure [26–28]. That is, plastic deformation occurs when the von Mises equivalent stress $\overline{\sigma}$ reaches the material yield strength σ_S. Firstly, the original purpose of the flexible cutting-tooth unit is to reduce the fatigue damage of the cutting tooth due to the impact load, so the von Mises stress is used to evaluate the vibration-reduction effect of the flexible cutting-tooth unit. Secondly, when cutting rock, the cutting teeth are in contact with the rock with the blade, so research into the distribution of the cutting load also focuses on the blade area. Furthermore, in the process of numerical simulation of rock breaking, the area of contact between the cutting teeth and the rock is constantly changing. Therefore, the instantaneous stress cannot accurately describe the stress characteristics of the tooth edge and the von Mises stress of the entire cutting process should be averaged.

Then, according to the research [29], under the action of a variable load, the weak area of the material is gradually damaged, and the damage accumulates to a certain extent; cracks are generated, and the cracks continue to grow leading to an unstable fracture. The characteristic is that the damage starts from the local area, accumulates continuously and eventually causes the overall damage. From the microscopic point of view, the von Mises stress value at the local point of the tooth edge is an important criterion for judging the vibration-reduction effect of the flexible cutting-tooth unit. In addition, the simulation results show that when the tooth-edge area is subjected to impact load, the cutting tooth interacts with the rear elastic element, which improves the stress value and distribution at the tooth edge to achieve a vibration-absorption effect. Therefore, the mean von Mises stress and the standard deviation of the stress in the tooth-edge area are also important criteria for assessing the vibration-reduction effect of the flexible cutting-tooth unit.

Therefore, some monitoring nodes are set at the edge of the tooth edge. The maximum value of the mean value of the von Mises stress at a single node is used to characterise the peak stress of the blade area. Moreover, the mean value and standard deviation of the von Mises stress of all nodes are used to characterise the stress of the entire blade area. Figure 12 shows the cutting-edge area and nodes of the selected cutting tooth.

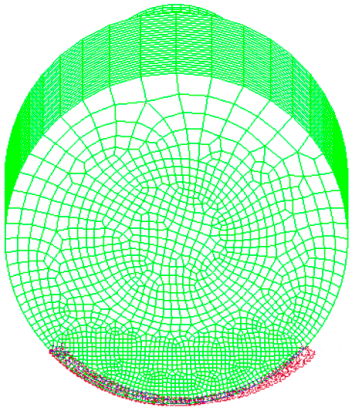

Figure 12. Cutting edge area and nodes of cutting tooth. (Scale: 2.5:1).

Part of the flexible and rigid scraping marks are shown in Figure 13a,b. It can be seen from the figures that in the front part of the scraping marks, the flexible scraping mark is irregular in relation to the rigid scraping mark. This is because when the cutting teeth are just in contact with the rock, an impact load is also generated, causing the tolerance phenomenon of flexible cutting and changing the depth of invasion. Although the force of the cutting tooth is in a state of dynamic equilibrium at this point, its working state is not normal and the reference value of this part of the data is not great. In the subsequent processing of the extracted stress data, only the relatively stable cutting-depth data of the rear section is retained. Correspondingly, when the data of rigid cutting is selected, the location and length of the data correspond to the stable section of the cutting depth of flexible cutting.

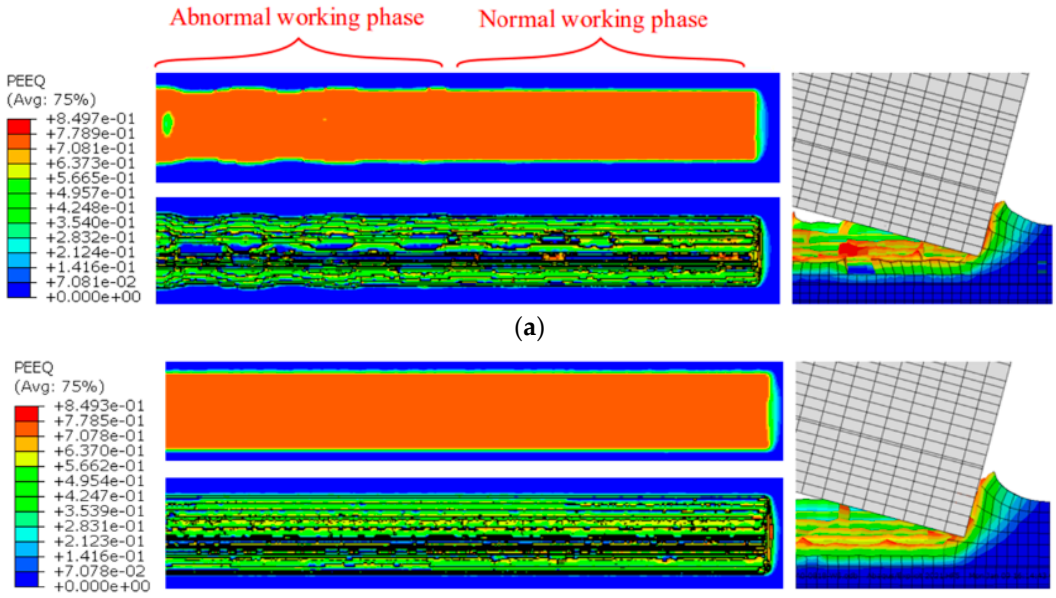

Figure 13. Comparison of flexible and rigid scraping marks. (**a**) Flexible cutting with preset depth of 1 mm. (**b**) The corresponding rigid cutting.

In the simulation experiment, the cutting depth of the rigid cutting is determined by the actual stable cutting depth of the flexible cutting. For example, when the rake angle is 15° and the disc-spring combination is A4, the preset cutting depth of the flexible cutting-tooth unit scraping limestone is 1 mm, but the actual cutting depth is 0.818 mm.

4.1. The Effect of the Cutting Depth

Under the condition that the front rake angle is 15° and the disc-spring combination is A4, Figure 14 shows the comparison of the average stress at the nodes when changing the cutting depth. It can be seen from Figure 15 that the peak stress of flexible cutting increases smoothly, and the peak stress of rigid cutting changes irregularly. However, under different cutting-depth conditions, the peak stress of rigid cutting is greater than that of flexible cutting, and flexible cutting reduces the peak stress at the cutting edge by 21.45–49.02%. Under the condition of a 1.3 mm preset cutting depth, the peak stress at the tooth edge of flexible cutting and rigid cutting are quite different. The flexible cutting is 476.98 MPa, but the rigid cutting is 935.69 MPa. The flexible cutting reduces the peak stress by 49.02%.

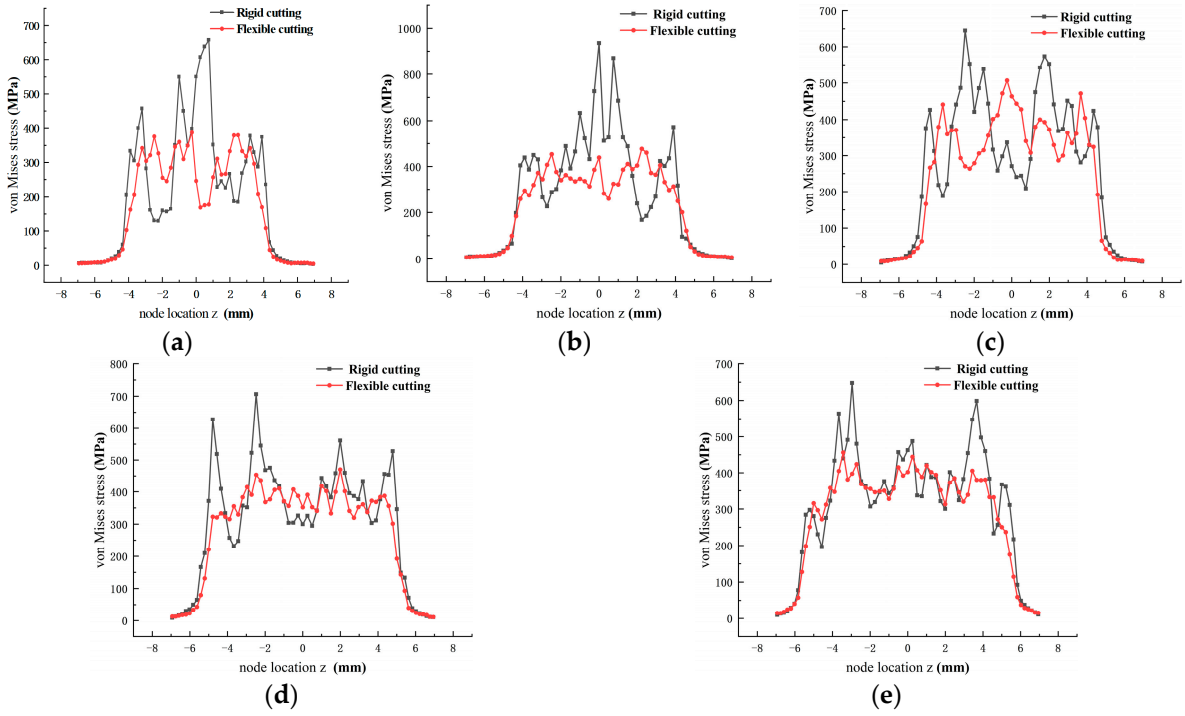

Figure 14. Comparison of von Mises stresses with varying preset cutting depths at tooth edge nodes. (**a**) 1 mm (**b**) 1.3 mm (**c**) 1.5 mm (**d**) 1.8 mm (**e**) 2 mm.

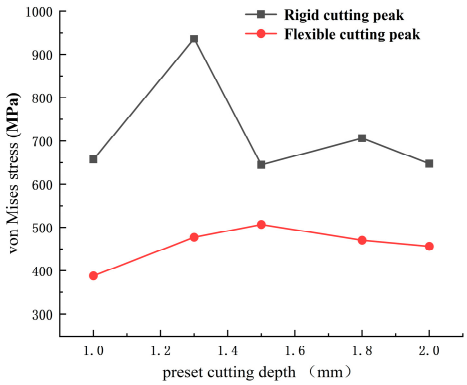

Figure 15. The peak values of von Mises stress with varying preset cutting depth.

It can be seen from Figure 16a that as the set cutting depth increases, the average stress at the tooth edge increases for both rigid and flexible cutting, but the average stress at the tooth edge area for flexible cutting is always less than that for rigid cutting. Flexible cutting reduces the average stress at the tooth edge by 9.42–17.8%. Compared with other

preset cutting-depth conditions, when the preset cutting depth is set to 1.3 mm, the average stress of rigid and flexible cutting is quite different. The average stress of flexible cutting is 211.99 MPa, but the average stress of rigid cutting is 257.9 MPa. Flexible cutting reduces the average stress by 17.8%. As shown in Figure 16b, as the preset cutting depth increases, the standard deviation of the blade stress in flexible cutting is always smaller than that in rigid cutting. When the preset cutting depth is set to 1.3 mm, the difference value of the stress standard deviation between rigid and flexible cutting edges is comparatively large, so the uneven distribution of tooth-edge stress is greatly improved by flexible cutting.

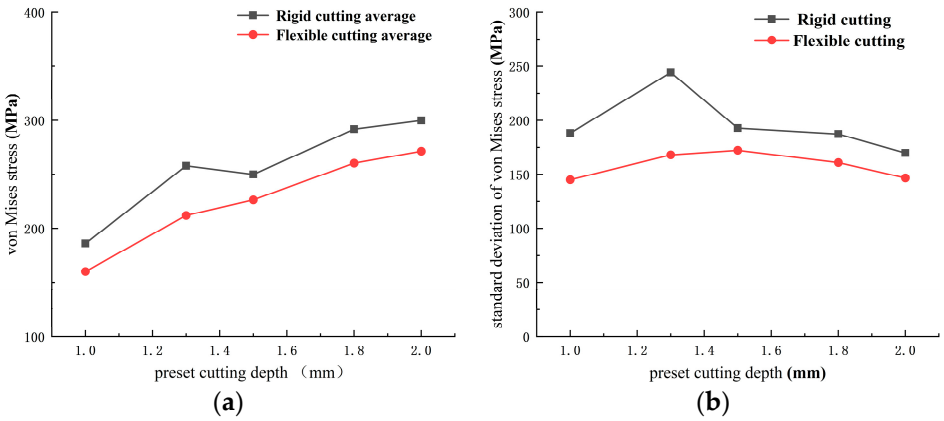

Figure 16. Comparison of von Mises stresses with varying cutting depths in the tooth-edge area. (**a**) The average values of von Mises stress (**b**) Standard deviation of von Mises stress distribution.

In summary, compared with rigid cutting, flexible cutting can make the stress distribution more uniform and also reduce the peak stress and average stress at the cutting edge. As the cutting depth increases, the peak-stress growth rate of flexible cutting is slower than that of rigid cutting. Under the condition of a 1.3 mm preset cutting depth, the differences between the peak stress and average stress of the two cutting models are large and the decreases are 49.02% and 17.8%, respectively.

4.2. The Effect of the Front Rake Angle

Under the condition that the disc-spring combination is A4 and the preset cutting depth is 1.5 mm, Figure 17 shows the comparison of the average stress at the nodes as the front rake angle changes. It can be seen from Figure 18 that the peak stress of rigid cutting first decreases and then increases, while the peak stress of flexible cutting changes more smoothly. Flexible cutting reduces the peak stress at the tooth edge by 20.51–44.54%. The peak stresses of the two cutting models are quite different at 10°. The flexible cutting is 427.01 MPa but the rigid cutting is 769.94 MPa. The flexible cutting reduces the peak stress by 44.54%.

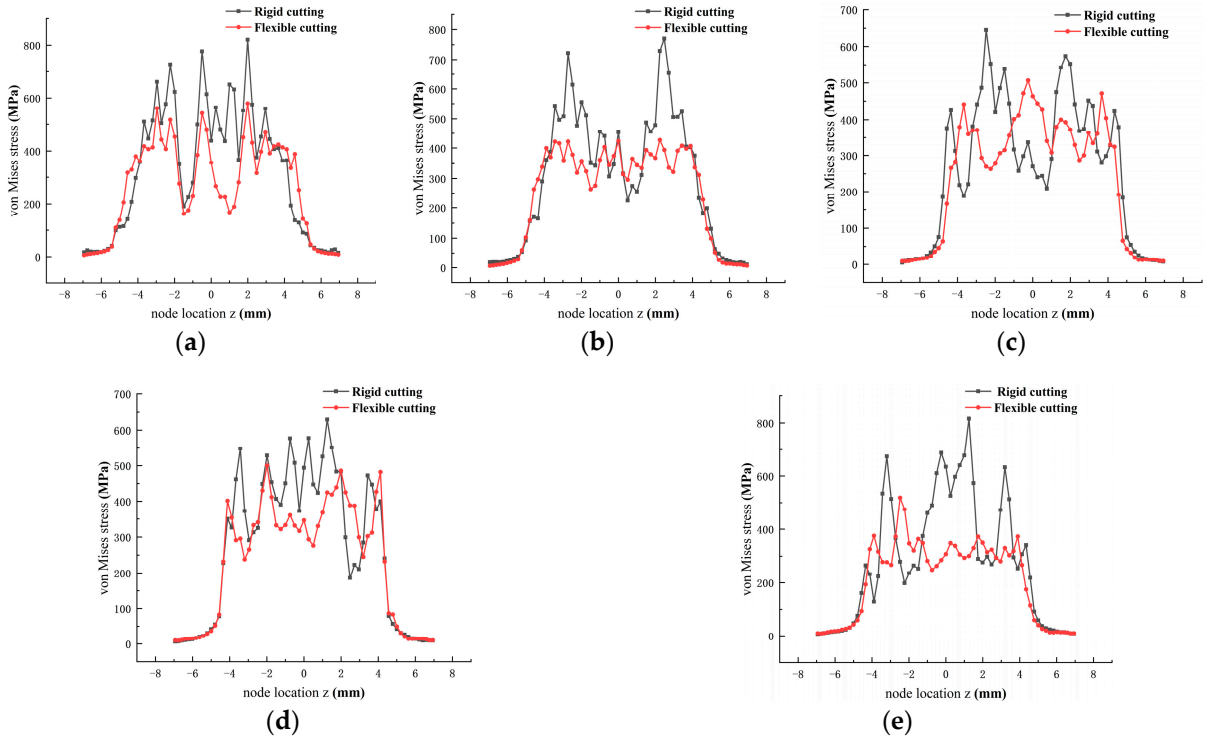

Figure 17. Comparison of von Mises stresses with varying front rake angle at tooth edge nodes. (**a**) 5° (**b**) 10° (**c**) 15° (**d**) 20° (**e**) 25°.

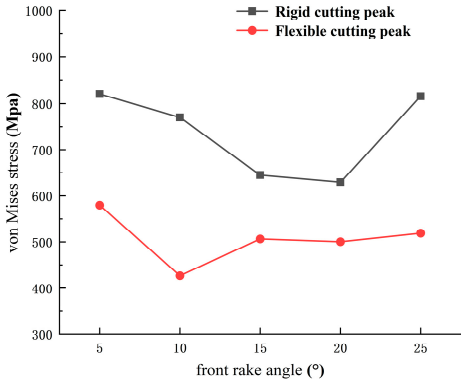

Figure 18. The peak values of von Mises stress with varying front rake angle.

From Figure 19a it can be seen that as the front rake angle increases, the average stress at the edge of the rigid cutting tooth first decreases and then increases. The average stress at the edge of the flexible cutting tooth decreases gradually. With flexible cutting, the average stress at the tooth edge decreases by 9.41–24.02%. The average stress of the cutting edge of the two cutting models is quite different at 25°. Flexible cutting is 199.19 MPa, while rigid cutting is 262.15 MPa, and flexible cutting reduces the average stress by 24.02%. It can be seen from Figure 19b that as the front rake angle increases, the standard deviation of the tooth-edge stress for flexible cutting is always smaller than that for rigid cutting. Under the condition of 10° rake angle, the difference value of stress standard deviation between rigid and flexible cutting edges is comparatively large, which indicates that flexible cutting has a better effect on improving the stress distribution of the cutting edge.

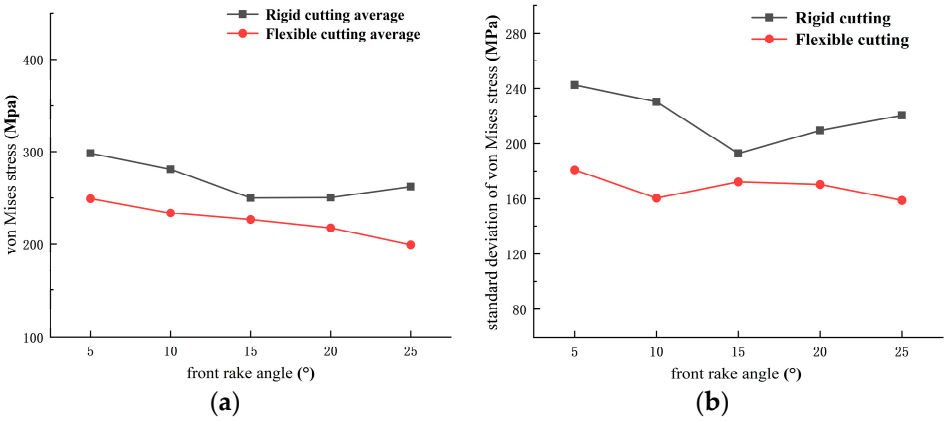

Figure 19. Comparison of von Mises stresses with varying front rake angle in the tooth-edge area. (**a**) The average values of von Mises stress (**b**) Standard deviation of von Mises stress.

In summary, under the condition of a 25° front rake angle, the average stresses of the cutting edge of the rigid and flexible cutting models are quite different, and the decrease reaches 24.02%. However, under the condition of a 10° front rake angle, the peak stresses of the cutting edge of the rigid and flexible cutting models are quite different, and the decrease reaches 44.54%. At this time, the difference value of the standard deviation of the stress distribution of the cutting edge between the two cutting models is larger. Therefore, the comprehensive vibration-reduction effect of the flexible cutting- tooth unit under the condition of a 10° forward angle is better.

4.3. The Effect of the Stiffness

Under the condition that the front rake angle is 15° and the preset cutting depth is 1.5 mm, Figure 20 shows the comparison of the average stress at the nodes by changing the disc-spring combination. From Figure 21a, it can be seen that the average stress of flexible cutting of the A2 and A4 disc-spring combinations is lower than the corresponding stress for rigid cutting, but the peak stress of A2 is higher than that corresponding to rigid cutting. The average stress on the blade for flexible cutting of the B4 and C4 disc springs are higher than that of the corresponding rigid cutting, but the peak stresses on the B4 and C4 disc springs is lower than that for corresponding rigid cutting. It can be seen from Figure 21b that the difference in stress standard deviation between rigid and flexible cutting is different for different disc-spring combinations. In comparison, the stress standard deviation is smaller and the stress distribution at the tooth edge is more uniform when using an A4 disc-spring combination. In addition, the difference between the stress standard deviations between the two cutting models using the A4 disc-spring combination is greater, indicating that the flexible cutting-tooth unit has a better effect on improving the uneven stress distribution.

In summary, if the stiffness of the elastic element is too high, the peak stress of the blade will be too high. On the other hand, if the stiffness is too low, the average stress on the blade will be too high and the stress distribution on the blade will be uneven. There is a suitable stiffness in the elastic element, which makes the peak stress and average stress at the cutting edge of the flexible cutting-tooth element perform better and the effect of improving the uneven stress distribution is better.

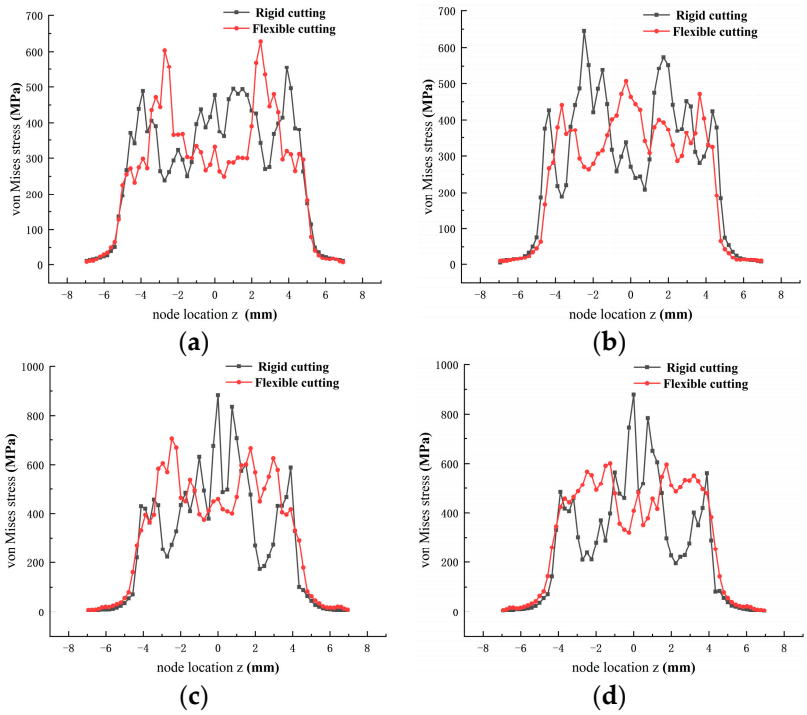

Figure 20. Comparison of von Mises stresses with varying disc-spring combinations at tooth edge nodes. (**a**) A2 (**b**) A4 (**c**) B4 (**d**) C4.

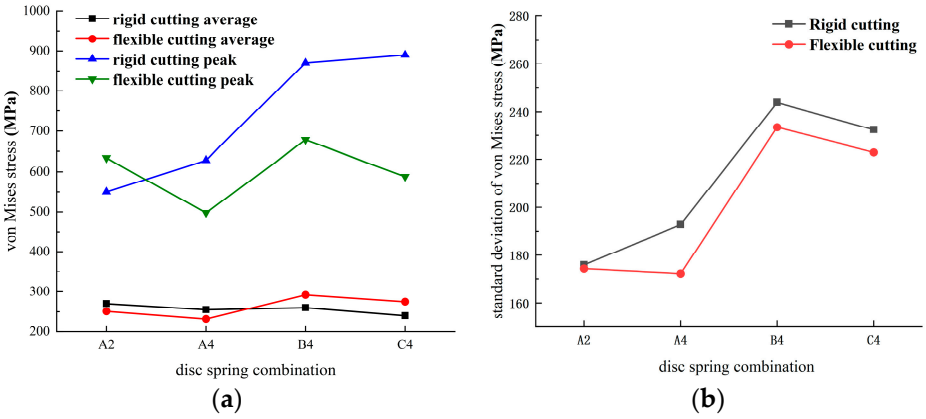

Figure 21. Comparison of von Mises stress data for variable types of disc-spring combinations in the tooth-edge area. (**a**) The average and peak values of von Mises stress (**b**) Standard deviation of von Mises stress.

5. Conclusions

The vibration-reduction mechanism of flexible cutting technology was theoretically analysed. The influence of cutting depth, front rake angle and stiffness of the elastic element on the vibration-reduction effect of the flexible cutting-tooth unit was discussed through the numerical simulation of rock breaking of the flexible cutting-tooth unit. The conclusions are as follows.

Firstly, fatigue failures such as tooth breakage, tooth fracture and delamination of the composite sheet are caused by impact dynamic load. The flexible cutting unit can achieve a good vibration-reduction effect by changing the cutting depth, increasing the number of teeth involved in cutting and extending the cutting-time history through adaptive retraction.

Secondly, compared with rigid cutting, flexible cutting can make the stress distribution at the cutting edge more uniform and reduce the peak stress and average stress. Under

the conditions of different cutting depths, the peak stress and average stress at the cutting edge decrease by 21.45–49.02% and 9.42–17.8%, respectively. As the cutting depth increases, the growth rate of the flexible cutting stress is slower than that of the rigid cutting stress. Under the condition of a 1.3 mm preset cutting depth, the peak stress and average stress between rigid and flexible cutting at the tooth edge are quite different, and the decrease is 49.02% and 17.8%, respectively.

Thirdly, under the condition of different front rake angles, the peak stress at the tooth edge is reduced by 20.51–44.54% and the average stress is reduced by 9.41–24.02%. Under the condition of a 10° front rake angle, the peak stress of the rigid and flexible cutting models at the tooth edge is quite different and the reduction reaches 44.54%. In addition, the difference in the standard deviation of the stress distribution of the tooth edge between the two cutting models is large under the same conditions as before, which indicates that flexible cutting has a better effect on improving the uneven stress distribution at the tooth edge. The overall vibration-reduction effect of the flexible cutting-tooth unit is better under the condition of 10° forward inclination compared to other angles.

Fourthly, if the stiffness of the elastic element is too high or too low, it will have a negative effect on the vibration-reduction effect of the flexible cutting unit. There is a suitable stiffness that makes the peak stress and average stress at the cutting edge of the flexible cutting-tooth unit better when working, and the effect of improving the uneven stress distribution is better.

Author Contributions: Conceptualization, H.R.; software, J.X.; investigation, S.Z., C.Z. and Q.Z.; writing—original draft preparation, X.J.; supervision, Y.Y. All authors have read and agreed to the published version of the manuscript.

Funding: This research was supported by the Open Fund of State Key Laboratory of Oil and Gas Reservoir Geology and Exploitation (Southwest Petroleum University), grant number (PLN2021-18) and Nanchong—Southwest Petroleum University Science and Technology Strategic Cooperation Project, grant number (SXHZ014).

Data Availability Statement: Not applicable.

Conflicts of Interest: The authors declare no conflict of interest.

References

1. Lv, M.R.; Shen, S.G. Research on stick-slip vibration dynamics of drill string. *J. Southwest Pet. Univ. Sci. Technol. Ed.* **2014**, *36*, 150–159.
2. Teng, X.Q.; Di, Q.F.; Li, N.; Chen, F.; Zhou, B.; Wang, M. Measurement and analysis of stick-slip vibration characteristics of drill string in ultra-deep wells. *Pet. Drill. Tech.* **2017**, *45*, 32–39.
3. Jia, X.L.; Zhong, X.L.; Liu, S.H.; Ji, Z.H. Analysis of stick-slip vibration characteristics of deep well drill string. *Oil Field Equip.* **2018**, *47*, 7.
4. Wang, G.M.; Li, D.; Ni, X.H. Research progress of special-shaped cutting teeth of PDC bit. *Oil Field Equip.* **2022**, *51*, 76–83.
5. Durrand, C.J.; Skeem, M.R.; Crockett, R.B.; Hall, H.R. Super-hard, thick, shaped PDC cuters for hard rock driling: Development and test results. In Proceedings of the 35th Workshop on Geothermal Reservoir Engineering, Stanford, CA, USA, 1–3 February 2010.
6. Zhao, D.P.; Ma, S.S.; Niu, T.J.; Li, S.C.; Zhang, C.L.; Fang, H.J. Performance characterization of curved polycrystalline diamond composite sheet for hard rock drilling. *Diam. Abras. Eng.* **2016**, *36*, 83–86.
7. Zhao, D.P.; Ma, S.S.; Niu, T.J.; Li, S.C.; Zhang, C.L.; Fang, H.J. Development of non-planar polycrystalline diamond compacts for oil drilling. *Diam. Abras. Eng.* **2017**, *37*, 49–52.
8. Liu, J.H.; Ling, W.X.; Wang, H. Study on rock breaking mechanism and field test of non-planar triangular PDC tooth. *Pet. Drill. Tech.* **2021**, *49*, 46–50.
9. Xu, G.P.; Liang, H.Y.; He, L.M.; Li, M.H. Development of high quality diamond compact (PDC) for oilfield drilling. *Min. Metall. Eng.* **2005**, *25*, 66–68+72.
10. Johnson, D.M.; Klug, F.J. Polycrystalline Diamond Compact Cutter with Reduced Failure during Brazing. U.S. Patent 6,042,463, 19 November 1998.
11. Gao, K.; Li, M.; Dong, B.; Sun, Y.H.; Sun, Y.; Liu, J. Bionic coupling polycrystalline diamond composite sheet drill bit. *Pet. Explor. Dev.* **2014**, *41*, 485–489. [CrossRef]
12. Yang, X.W.; Peng, Q.; Feng, X.; Liu, Y.; Ke, X.H.; Liu, B.C.; Tu, J.B. Numerical simulation of matrix interface shape on PDC residual stress. *China Pet. Mach.* **2023**, *51*, 82–88.

13. Han, L.J.; Yang, C.X. Key drilling and completion technologies of shale oil horizontal wells in Jiyang Depression. *Pet. Drill. Technol.* **2021**, *49*, 22–28.
14. Wang, M. Optimization design and application of PDC bit in complex lithology formation. *West-China Explor. Eng.* **2023**, *35*, 70–72.
15. Jaggi, A.; Upadhaya, S.; Chowdhury, A.R. Successful PDC/RSS Vibration Management Using Innovative Depth-of-Cut Control Technology: Panna Field, Offshore India. In Proceedings of the SPE/IADC Drilling Conference and Exhibition, Amsterdam, The Netherlands, 20–22 February 2007.
16. Jain, J.R.; Ledgerwood, L.W.; Hoffmann, O.J.; Schwefe, T.; Fuselier, D.M. Mitigation of Torsional Stick-Slip Vibrations in Oil Well Drilling through PDC Bit Design: Putting Theories to the Test. In Proceedings of the SPE Annual Technical Conference and Exhibition, Denver, CO, USA, 30 October–2 November 2011.
17. Zheng, J. New progress of diamond bit abroad. *China Pet. Mach.* **2016**, *44*, 31–36.
18. Jain, J.R.; Ricks, G.; Baxter, B.; Vempati, C.; Peters, V.; Bilen, J.M.; Spencer, R.; Stibbe, H. A Step Change in Drill-Bit Technology With Self-Adjusting Polycrystalline-Diamond-Compact Bits. Soc. *Pet. Eng. Drill. Complet.* **2016**, *31*, 286–294. [CrossRef]
19. Kenneth, E.; Russell, S.C. Innovative Ability to Change Drilling Responses of a PDC Bit at the Rigsite Using Interchangeable Depth-of-Cut Control Features. In Proceedings of the IADC/SPE Drilling Conference and Exhibition, Fort Worth, TX, USA, 1–3 March 2016.
20. Si, N.; Deng, H.; Li, J.; Pi, G.L. Baker Hughes adaptive PDC bit. *Fault-Block Oil Gas Field* **2017**, *24*, 125–130.
21. Zhu, X.H.; Tang, L.P.; Meng, P.P.; Wang, P.; Wang, Y. Mechanism analysis of stick-slip vibration of PDC bit. *Oil Field Equip.* **2012**, *41*, 13–16.
22. Fu, M.; Li, J.H.; Wu, Y.F.; Li, Y.R. Simulation and mechanism analysis of stick-slip vibration characteristics of drill string. *J. Northwest. Polytech. Univ.* **2016**, *41*, 467–472.
23. He, Z.G.; Shi, L.B.; Li, L.; Kong, L.X.; Kong, L.L.; Zhang, X.N.; Liu, X.Y. Study on stick-slip vibration mechanism based on finite element simulation of single-tooth rock breaking. *China Pet. Mach.* **2021**, *49*, 17–26.
24. Yang, Y.X.; Ren, H.T.; Lin, Z.H.; Wu, M.; Yang, Y. Cutting Teeth and Adopt Diamond Bit of This Cutting Teeth with Damping Function. CN CN208137865U, 2018.
25. Zhou, R.; Zhang, L.H.; He, B.Y.; Liu, Y.H. Numerical simulation of residual stress field in green power metallurgy compacts by modified Drucker–Prager Cap model. *Nonferrous Met. Soc. China Trans.* **2013**, *23*, 2374–2382. [CrossRef]
26. Luan, M.T.; Yang, X.H.; Yang, Q.; Fan, C.; Ye, X.J. The maximum Mises stress composite fracture criterion considering the three-dimensional stress effect. *Rock Soil Mech.* **2006**, *27*, 1647–1652.
27. Jin, Y.S.; Li, L. Study on Von Mises Stress Process of Structure under Random Vibration Loading. *Chin. J. Appl. Mech.* **2004**, *21*, 13–16+157–158.
28. Xue, G. Analysis of mechanical properties of welded joints based on Mises yield criterion and I_1 fracture criterion. *Dev. Appl. Mater.* **2022**, *37*, 1–10.
29. Chen, X.H.; Xu, Y.D.; Song, Y.K.; Han, J.G.; Wu, H.Y.; Cao, Z.X.; Shao, Z.W.; Chen, X.H. Effect of loading mode on fatigue performance of needle valve. *Ordnance Mater. Sci. Eng.* **2023**, *46*, 118–124.